Running Head: Dynamics of conifer encroachment into aspen stands in the Lake Tahoe Basin

Understanding Rates and Drivers of Conifer Encroachment in Aspen Stands Throughout the Lake Tahoe Basin During the Past 35 Years

Final Report for Nevada Division of State Lands
Lake Tahoe License Plate Program
April 30, 2021

Thomas E. Dilts[1], Tyler K. Refsland[1], Jonathan A. Greenberg[1], & J. Hall Cushman[2]

Department of Natural Resources & Environmental Science
University of Nevada, Reno, NV 89557

[1]co-PI; [2]PI (jhcushman@unr.edu)

Understanding Rates and Drivers of Conifer Encroachment in Aspen Stands Throughout the Lake Tahoe Basin During the Past 35 Years

Thomas E. Dilts, Tyler K. Refsland, Jonathan A. Greenberg, & J. Hall Cushman
Department of Natural Resources & Environmental Science
University of Nevada, Reno, NV 89557

Final Report for Nevada Division of State Lands
Lake Tahoe License Plate Program
April 30, 2021

Abstract

Human-driven changes in disturbance regimes affect forest structure and composition and threaten the provision of critical ecosystem services. Fire suppression promotes the dominance of later successional tree species at the expense of species that benefit from periodic disturbance. Quaking aspen (*Populus tremuloides*), the most widely distributed tree species in North America, is a foundation tree species whose persistence in the Sierra Nevada is threatened by extensive fire suppression and lack of stand-replacing disturbance. By digitizing aspen stands throughout the Lake Tahoe Basin (LTB) using high-resolution imagery and modeling trends in conifer encroachment in aspen stands using the Landsat archive, we sought to address the following research questions: 1) What is the rate of conifer encroachment within aspen stands in the LTB from 1985 to 2020? 2) How do the rates of conifer encroachment vary spatially across the LTB, both within and among aspen stands? 3) What biotic and abiotic variables predict the rate of conifer encroachment into aspen stands? 4) Are there environments in the LTB that support aspen populations but preclude conifer encroachment?

We found that conifer cover within aspen stands increased by an average of 2.6% across the LTB between 1985 and 2020. The rates of increase were spatially heterogeneous, but also positively associated with initial (1985) conifer cover, negatively associated with mean annual precipitation, and dependent on the relative dominance of neighboring conifers and aspen. Although we did not find strong evidence of sites that were resistant to conifer encroachment, the overall spatial heterogeneity in conifer encroachment across the LTB showed cases (e.g., large aspen stands near Marlette Lake) where conifer expansion is substantially slower than elsewhere. Based on our results, we provide a set of interactive, web-based maps that land managers can use to identify aspen stands throughout the LTB that may be most susceptible to conifer encroachment. Without management intervention, we project that conifer encroachment will continue to increase across most of the LTB, threatening the unique habitats and ecosystem services that aspen provides.

Keywords: Conifer encroachment; disturbance; fire suppression; Lake Tahoe Basin; mixed conifer forests; *Populus tremuloides*; Sierra Nevada; succession.

Introduction

Hotter temperatures and shifts in rainfall patterns due to climate change are increasing drought stress and mortality in forests, especially in the western U.S. (Breshears et al. 2005; van Mantgem et al. 2009; Allen et al. 2010, 2015). Elevated rates of tree mortality threaten critical ecosystem services provided by forests, including timber production, water purification, recreational use and their central role as carbon sinks (Bonan 2008; Pan et al. 2011; Trumbore et al. 2015). However, our ability to predict forest susceptibility to ongoing climate change is limited by our understanding of how drivers of mortality vary and interact across heterogeneous landscapes and over long time periods. This limitation has made it challenging to identify forest stands that are in decline and may require active management by agency professionals.

Quaking aspen (*Populus tremuloides*) is the most widespread tree species in North America but is experiencing substantial stress-induced declines across many regions of the western U.S. (Rehfeldt et al. 2009; Worrall et al. 2008, 2010, 2013; Huang and Anderegg 2012; Zegler et al. 2012). In the Sierra Nevada Mountains, aspen stands are at risk primarily due to climate change, fire suppression and conifer encroachment (Jones et al. 2005; Sheppard et al. 2006; Stephens et al. 2007; Berrill and Dagley 2012; Krasnow et al. 2015). These declines are particularly concerning given that aspen stands act as natural firebreaks (Smith et al. 1993; Carlson et al. 2011), have major effects on carbon sequestration and hydrological cycles, and support exceedingly high levels of biodiversity relative to surrounding coniferous forests (Kuhn et al. 2011). Because of these critical impacts as well as their aesthetic value, aspen stands have been designated as Ecologically Significant Areas in the Lake Tahoe Basin (hereafter referred to as LTB; Manley et al. 2000).

Given the importance of aspen in the LTB, it is critical to quantify the long-term dynamics of conifer encroachment in aspen stands and to identify the factors that influence rates of this encroachment. The resilience of aspen stands to conifer encroachment is expected to be spatially and temporally heterogeneous across landscapes (Kashian et al. 2007; Strand et al. 2009; McCullough et al. 2013), but few studies have attempted to quantify this (Strand et al. 2009). Based on more general studies of aspen recruitment, we would predict that conifer encroachment rates into aspen stands would be greater 1) in upland than wet microsites near springs, streams and meadows where aspen is most competitive (Strand et al. 2009); 2) in flatter sites that lack natural barriers (e.g., talus deposits) to herbivory (Ripple and Larsen 2001) and conifers recruitment (Turner et al. 2003); 3) at lower elevations and along south-facing slopes where warmer and drier conditions may increase the susceptibility of aspen to stress-induced mortality (e.g., Gitlin et al. 2006; Huang and Anderegg 2012; Dudley et al. 2015); and 4) in aspen stands near conifers crowns (Berrill and Dagley 2012), especially shade-tolerant fir species (Pierce and Taylor 2010). Testing these predictions will be critical for understanding the dynamics of forests in the LTB and for effectively managing these important natural resources.

Here, we summarize research that has evaluated the dynamics of aspen and associated conifers within the LTB using remote sensing approaches. Our project has addressed the following questions:

1) What are the rates of conifer encroachment within aspen stands in the LTB from 1985 to 2020?
2) How do the rates of conifer encroachment vary spatially across the LTB, both within and among aspen stands?
3) What biotic and abiotic variables predict the rate of conifer encroachment into aspen stands?
4) Are there environments in the LTB that support aspen populations but preclude conifer encroachment?

Our hope is that answers to these questions will contribute significantly to the long-term health and persistence of aspen populations in the LTB and support management efforts by identifying aspen stands that are most likely to benefit from restoration actions.

Methods

Study system

Our study area consisted of the entire landscape located within the Lake Tahoe Basin (LTB; 39°N 120°W) of the Sierra Nevada. Lake Tahoe is a high-elevation lake (1,889 m) surrounded by mostly coniferous forest, montane chaparral, alpine vegetation, and bare rock with elevations up to 3316 m. Within the LTB, the U.S. Forest Service is the largest land holder, with 78% of the basin under its charge. Other important land owners include California and Nevada State Parks as well as several smaller private land holders. The climate in the LTB is montane Mediterranean (Koeppen Csc), with cool wet winters (average January minimum is -7.2° C), warm dry summers (average July maximum is 25° C), and the vast majority of precipitation (75% of 86.8 cm) being delivered as snow during the winter and spring months.

Quaking aspen is distributed throughout the LTB from 1,897 up to 2,716 m and occupies a range of environmental settings that include riparian zones and talus slopes. In addition, aspen occurs as both nearly homogenous stands as well as mixed with conifers. Although aspen stands represent just over 1% of the total land area in the LTB, the species is vitally important as habitat for a wide range of species including understory plant diversity (Kuhn et al. 2011), invertebrates (Bailey and Whitham 2002), and passerine birds (Richardson and Heath 2004; Richardson and Vanderwall 2007).

Delineation of aspen stands and conifers-within-aspen using high-resolution imagery

Although aspen has been studied in the LTB (Berrill et al. 2017; Dagley et al. 2020), and is a vegetation type that land management agencies are actively trying to maintain and promote because of their ecosystem services (Manley et al. 2000), consistent and detailed maps of aspen stand boundaries are lacking in this region. To ensure that change detected from coarse-scale satellite imagery (i.e., Landsat) was not ascribed to neighboring vegetation communities, such as adjacent coniferous forest, meadows, or other riparian deciduous communities (e.g., willows, cottonwoods), we created our own detailed map of aspen stands using high-resolution imagery in a Geographic Information System. These aspen maps were used to ensure that only pixels located entirely within aspen were used in model training for the subsequent change-detection analysis.

To create the detailed maps demarcating the outside boundary of aspen stands, we used a variety of high-resolution images in both ArcMap 10.7.1 (Esri 2019) and Google Earth Pro 7.3.3 (Google 2017). Imagery that was used included the WorldView-2 (Google Inc.)), USDA National Agriculture Imagery Program (NAIP) (USDA 2017), and the LTB LIDAR dataset of August 11, 2010 (Romsos 2011). We began mapping using known existing aspen stands which included the Aspen Delineation Project (Stermer 2011), the Lake Tahoe Basin Management Unit (LTBMU) vegetation map (Ottmar and Safford 2011), and point locations provided to us by the US Forest Service LTBMU (Stephanie Coppetto, pers. comm.). Criteria for identifying aspen stands included the white bark of leaf-off aspen in high-resolution imagery, the presence of downed wood in the understory, presence of shadows indicating taller trees as compared to riparian shrubs, presence of yellow foliage in fall imagery, and height and intensity of LIDAR indicating tree stature rather than shrub stature. In order to be considered an aspen patch, we required that more than one aspen tree be visible in imagery. Although we began our delineation in areas of known aspen stands, we ultimately searched the entire land base of the LTBMU. All mapping was first done by a single trained GIS analyst (Hannah Williams) and follow-up mapping and corrections were performed by T. Dilts.

High-resolution leaf-off imagery provided a unique opportunity to identify conifers within the understory of aspen, which allowed us to directly map conifer encroachment. A subset of stands with high-quality leaf-off imagery (n = 133) located in the northeast quadrant of the LTB from Kings Beach, CA to Zephyr Cove, NV were selected for detailed conifer mapping. Using the high-resolution imagery, we mapped 5,706 polygons representing individual conifers or groups of coniferous trees with a minimum mapping unit of 0.4 m^2. Within the selected polygons, we did a complete inventory and we mapped conifer polygons such that they extended outside of our stand polygons in order to minimize edge issues.

Aspen stand maps were validated in the field using 122 randomly selected aspen points within 200 m of a road, paired with 122 non-aspen points along the eastern half of the LTB (Incline Village, NV to South Lake Tahoe, CA). Sites were located using a Trimble GeoXT. For sites that were mapped as aspen, but consisted of other vegetation, we recorded the alternative vegetation present.

Mapping conifer cover in aspen stands using Landsat imagery from 1985 to 2020

Using the mapped conifer polygons from the previous step as training data, and Landsat spectral bands as predictor variables, we developed annual-resolution models of conifer cover within aspen stands for 2018 and extrapolated those models to cover the 1985 to 2020 time period. Using the Mann-Kendall trend test, we mapped slopes in the trend of conifer cover within aspen stands at the 30-m pixel scale.

Using the aspen stands from the previous step, we identified 133 stands with mapped conifers and 1004 Landsat pixels that were entirely within the boundaries of the mapped aspen stands. We randomly divided the data into training (n=500) and validation (n=504). For each training point, we used Landsat spectral bands (blue, green, red, near-infrared, shortwave infrared 1, and shortwave infrared 2; Table 1) as well as the Normalized Difference Vegetation Index (NDVI;

Tucker 1979) and Normalized Difference Wetness Index (NDWI; Gao 1996). Using Climate Engine (Huntington et al. 2017), a website that runs on Google Earth Engine (Gorelick et al. 2017), we developed annual-resolution mean image composites of Landsat TM, ETM+, and OLI using winter imagery (December 1 through April 30). Winter imagery was selected for this analysis because it avoided some of the confounding issues that we encountered with summer and fall imagery. With summer imagery, we encountered high variability in canopy greenness, likely caused by disease or insect defoliation (e.g., satin moth; Enders 2021), which confounded estimates of conifer cover through time. Likewise, autumn imagery was subject to late-season defoliation by satin moth (Enders 2021) as well as inter-annual variation in leaf senescence, leading to large fluctuations in predicted conifer cover from year to year. The use of winter imagery circumvented these issues, and had the additional benefit of maximizing the contrast between conifers, which are photosynthetically active during the winter, and an understory that is photosynthetically inactive and frequently covered in snow. Imagery from 1984 was omitted due to excessive cloud cover.

Table 1. *Spectral bands of Landsat TM (1985-2011), ETM+ (1999-2020), and OLI (2013-2020) in micrometers used in this study. NIR = near-infrared. SWIR1/2 = shortwave infrared. We did not use the coastal/aerosol band (0.433 – 0.453) or cirrus band (1.360 – 1.390) of OLI or the panchromatic band of any sensor.*

	Blue	Green	Red	NIR	SWIR1	SWIR2
TM	0.45–0.52	0.52–0.60	0.63–0.69	0.76–0.90	1.55–1.75	2.08–2.35
ETM+	0.45–0.52	0.52–0.60	0.63–0.69	0.77–0.90	1.55–1.75	2.09–2.35
OLI	0.45–0.51	0.53–0.59	0.64–0.67	0.85–0.88	1.57–1.65	2.11–2.29

To model the fractional cover of conifers in aspen pixels, we overlaid the conifer polygons with Landsat footprint polygons and calculated the proportion conifer within each Landsat pixel. We used the randomForest package in R (Liaw and Wiener 2002) to model the proportion conifer using regression trees using default parameters (ntrees=500, mtry=2). Models were tested on 504 randomly-withheld validation points. We extrapolated model predictions both forward and backward in time to cover the entire time period from 1985 to 2020, with 2018 serving as the reference year in which both training and validation data were drawn. Although we intended to validate our predictions using historical, high-resolution color aerial photographs, there was no suitable, color imagery available for the area and time period of interest.

Because of differences in the timing of the imagery due to cloud cover and seasonality of vegetation, as well as differences in the wavelengths among the different Landsat sensors (TM, ETM+, OLI), time series can be noisy (Kennedy et al. 2010). To reduce the noise in the time series and to generate more ecologically-realistic patterns through time (e.g., conifers are expected to increase gradually), we used a median filter with the focal year's conifer cover as well as one year previous and one year after. Using the entire 35-year period, we calculated the Mann-Kendall correlation, Sen's slope, and p-values for each pixel using the spatialEco package in R (Evans 2020). Overlaying the statistical significance of the Mann-Kendall correlation (alpha=0.05) with the slope, we generated three classes of change – not significant, significant declines, and significant increases. Pixels with significant increases were further analyzed to determine the potential drivers of change.

Modeling environmental settings that are associated with the amount of conifer

To understand the abiotic factors and stand characteristics that might lead to differences in conifer encroachment rates, we compiled a range of topographic, soil, climatic, vegetation variables (Table 2) and used these to create a predictive model of conifer encroachment within aspen stands. Topographic variables included slope in degrees, Topographic Position Index calculated at 990-m scale (Weiss 2001), Topographic Wetness Index (Beven and Kirkby 1979), Heat load Index (McCune and Keon 2002), and a modified version of the Vector Ruggedness Measure that removes underlying topographic variation in order to obtain better estimates of ruggedness in drainages and ridgelines (Sappington et al. 2007). All of the soil variables were derived from POLARIS (Chaney et al. 2016), a gridded product trained on USDA SSURGO soil data (USDA 2014). Soil variables included the proportion of sand, silt, clay, and organic matter, soil pH, available water capacity, and depth to restrictive layer. Climatic variables included mean annual temperature and precipitation, both derived from PRISM 30-year normals calculated from 1981-2010 (Daley et al. 1994). In the LTB, mean annual temperature varies primarily with elevation whereas precipitation is greatest on the west shore of the lake and is much lower on the eastern shore.

Vegetation variables described both the aspen stand itself as well as neighboring vegetation communities. Shape Index (Forman and Godron 1981) was used to describe the elongation of aspen patches. Proximity to the nearest aspen patch was calculated based on Euclidean distance using ArcGIS Spatial Analyst (Esri 2019). The remaining vegetation variables were calculated at three spatial scales (30, 510, and 990 m), as multi-scale models have frequently been shown to be more predictive and more interpretable than single-scale models. We calculated aspen area at each of the three scales using our mapped patches derived from high-resolution imagery. The vegetation variables were derived from the LTB Management Unit vegetation map (Ottmar and Safford 2011) and included red fir, mixed conifer, yellow pine, white pine, chaparral, and lodgepole pine. Total canopy cover was derived from LTB LIDAR dataset from 2010. Finally, we used 1985 conifer cover in order to determine whether there may be a relationship between initial conifer cover and trend in conifer encroachment.

The response variable was derived from the Sen slope raster for all significantly increasing pixels and included pixels adjacent to neighboring vegetation types (unlike our remotely sensed model of conifer cover that only included pixels entirely within aspen) (n=3,332). We used the randomForest package in R (Liaw and Wiener 2002) to model conifer encroachment rates using regression trees with default parameters (ntrees=500, mtry=2). To ensure a parsimonious model and to facilitate ecological interpretation of the partial response curves we used a three-step procedure to remove variables (Table 2). First, we ran the model including all variables. Second, we removed all variables that contributed less than 1% to the model as measured by the mean decrease in accuracy from the Random Forest. If multiple scales of the same variable were present, we removed the variable that contributed the least to the model. We re-ran the Random Forest with the reduced set of variables, successively removing variables and plotting the out-of-bag error against the number of variables, which indicated that the model did not improve with the addition of more than six variables. Finally, we ran the Random Forest in regression-tree mode with conifer cover change as the response variable and our reduced variable set of six variables.

Table 2. *Variables included in each iteration of the prediction of conifer encroachment rate (columns 5 and 6) and in each iteration of the encroachment occurrence model (columns 7 and 8).*

	Name	Description	Source	2nd	Final	2nd	Final
soils	sand	percent sand	POLARIS	Y		Y	
	silt	percent silt	POLARIS	Y	Y	Y	Y
	clay	percent clay	POLARIS	Y		Y	
	OM	percent organic matter	POLARIS	Y		Y	
	pH	soil pH	POLARIS	Y	Y	Y	
	AWC	available water capacity of the soil	POLARIS	Y		Y	Y
	resdt	depth to restrictive layer	POLARIS			Y	
topo	slope	slope in degrees	NED	Y		Y	
	ruggedness	topographic ruggedness	Dilts in prep	Y		Y	
	TPI	Topographic Position Index at 990 m	Weiss 2001	Y		Y	
	TWI	Topographic Wetness Index	Beven and Kirkby 1979	Y			
	Heat Load	Heat Load Index (solar radiation)	McCune and Keon 2002	Y		Y	
climate	precipitation	Annual precipitation	PRISM	Y	Y	Y	Y
	temp	Mean annual temperature	PRISM	Y	Y	Y	Y
vegetation	Conifer 1985	conifer cover in 1985	our model	Y	Y	Y	
	aspenarea3	percent aspen within 30 meter radius	our digitizing				
	aspenarea5	percent aspen within 510 meter radius	our digitizing	Y	Y		
	aspenarea9	percent aspen within 990 meter radius	our digitizing			Y	Y
	Aspen proximity	distance to the nearest other aspen stand	our digitizing				
	Aspen shape	aspen stand shape index	Forman and Godron 1986				
	canopy30m	percent canopy within 30 meter radius	Tahoe LIDAR 2010				
	Canopy90m	percent canopy within 90 meter radius	Tahoe LIDAR 2010			Y	Y
	canopy510m	percent canopy within 510 meter radius	Tahoe LIDAR 2010	Y	Y		
	canopy990m	percent canopy within 990 meter radius	Tahoe LIDAR 2010				
	Chapparal 3	percent chapparal within 30 meter radius	CALVEG				
	Chapparal 5	percent chapparal within 510 meter radius	CALVEG				
	Chapparal 9	percent chapparal within 990 meter radius	CALVEG	Y		Y	
	Lodgepole 3	percent lodgepole pine within 30 meter radius	CALVEG				
	Lodgepole 5	percent lodgepole pine within 510 meter radius	CALVEG	Y			
	Lodgepole 9	percent lodgepole pine within 990 meter radius	CALVEG			Y	
	Mixed 30	percent mixed conifer within 30 meter radius	CALVEG				
	Mixed 510	percent mixed conifer within 510 meter radius	CALVEG				
	Mixed 990	percent mixed conifer within 990 meter radius	CALVEG	Y	Y	Y	Y
	Redfir 30m	percent red fir within 30 meter radius	CALVEG				
	Redfir 510m	percent red fir within 510 meter radius	CALVEG				
	Redfir 990m	percent red fir within 990 meter radius	CALVEG			Y	
	White 30	percent white pine within 30 meter radius	CALVEG				
	White 510	percent white pine within 510 meter radius	CALVEG				
	White 990	percent white pine within 990 meter radius	CALVEG				
	Yellow 30	percent yellow pine within 30 meter radius	CALVEG				
	Yellow 510	percent yellow pine within 510 meter radius	CALVEG				
	Yellow 990	percent yellow pine within 990 meter radius	CALVEG	Y		Y	Y

Comparing the ecological niche of invaded aspen vs. non-invaded aspen

In addition to understanding the rate of conifer encroachment within aspen, we also sought to understand whether certain topoclimatic settings for aspen might be less susceptible to encroachment than others. Using the results of the Mann-Kendall trend analysis, we classified all aspen pixels into two categories: 1) statistically-significant increases and 2) decreases or statistically-insignificant increases. We used the same 42 predictor variables as in the conifer encroachment model and applied a similar variable-reduction procedure that involved fitting an initial model with all variables followed by a second model where variables contributing less than 1% to the model, as measured by mean decrease in accuracy, were removed as were

variables that represented the same vegetation type but at different spatial scales. Finally, we used an iterative procedure to cull variables where we ranked variables from the second model using mean decrease accuracy, iteratively added variables based on their ranking starting with the most important variable, and assessed the error rate. We stopped adding variables once additional ones no longer increased the predictive accuracy of the model.

Results

Aspen stands and conifers-within-aspen from high-resolution imagery

Our detailed mapping using high-resolution imagery found aspen stands occupied 863 ha, comprising approximately 1.06% of the total land area within the LTB. The average size of aspen stands was 1.63 ha and there was a highly skewed size distribution, with 90% of stands encompassing less than 3.51 ha. The largest stand was 33.67 ha and is located adjacent to Snow Valley Peak. There were a total of 529 aspen stands identified in the LTB, with 54.5% of them in California and the remainder in Nevada. Field validation showed that the map of digitized aspen stands was 87.7% accurate, with 100% of the non-aspen points being correctly classified and 30 points incorrectly mapped as aspen. All cases of false positives were instead other deciduous riparian tree species, most commonly willows (*Salix* spp.) followed by black cottonwood (*Populus balsamifera* ssp. *trichocarpa*) and mountain alder (*Alnus incana* ssp. *tenuifolia*). A total of 5,076 polygons representing individual conifers and groups of conifers were mapped within aspen stands. Of the 133 aspen stands within which conifers were mapped, conifers comprised a total of 32.11 ha (3.72%) of the total area occupied by aspen in the LTB. On average, conifers comprised 10.7% of the area within each aspen stand.

Landsat-based estimates of conifer cover in aspen stands from 1985 to 2020

The Landsat-based remote sensing model of 2018 conifer cover within aspen stands explained 28.5% of the variation in conifer cover compared to the digitized mapping based on high-resolution imagery. The Landsat-based model had a bias of 1.24% such that when predicting

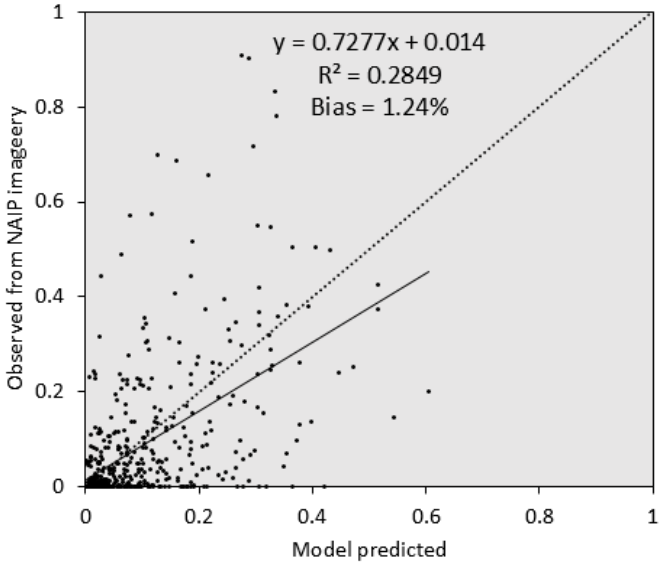

Figure 1. *Relationship between 2018 digitized estimates of conifer cover within aspen stands from high-resolution imagery and predicted conifer cover from the Landsat spectral indices/bands. The dashed line is the 1:1 line. The solid line is the least-squares line fit to the digitized reference data.*

conifer cover greater than 5%, the model tended to overpredict relative to the digitized data (Figure 1). The normalized root mean squared error was 13.94%. The distribution of conifer cover values in the modeled data differed from the source data in some important ways. First, predicted values tended to have fewer very high or very low values, which is evident in the range of data on the y-axis of Figure 2 being much greater than on the x-axis. Second, values of zero are much more common in the scatterplot on the y-axis (observed) compared to the x-axis (predicted). These differences manifest themselves in the spatial predictions of conifer cover. For example, predicted maps of conifer cover in aspen stands visually resemble the patterns of mapped conifer cover, but appear fuzzy because true zero values are very difficult to predict (Figure 2). In contrast, pixels with zero conifer cover are much more common and visually apparent in the maps.

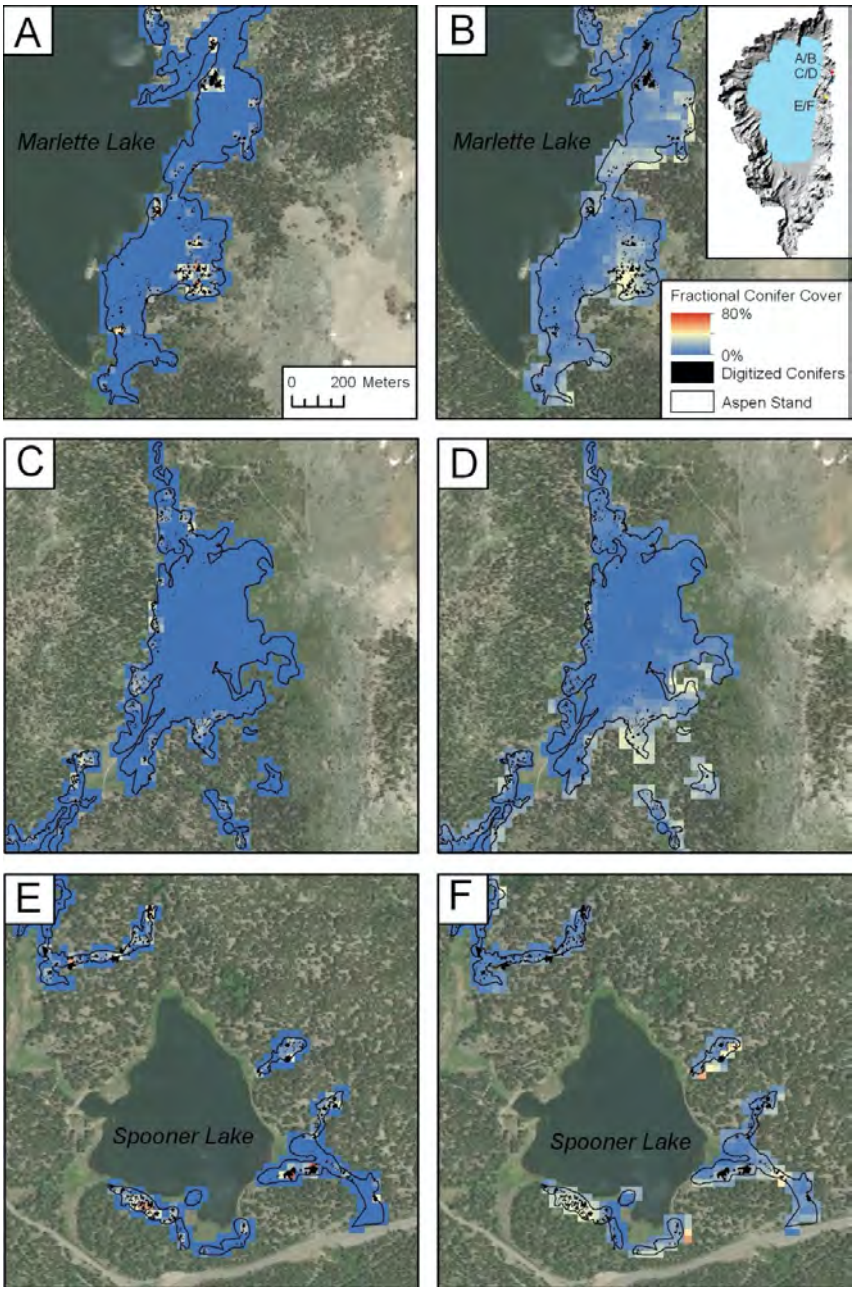

Figure 2. *Estimates of fractional conifer cover within aspen stands in 2018 as digitized from high-resolution imagery (A,C,E) and modeled from Landsat spectral bands (B, D, F).*

Across all aspen stands in the LTB, our Landsat-based predictions of 2018 conifer cover showed an average of 16.1% (± 12.4% SD) of the total area in each aspen stand was coniferous, with a maximum predicted conifer cover of 80.2%. The distribution of predicted conifer cover was highly skewed, with 25% of cells having cover less than 5.8% and 25% having cover greater than 25%. The median conifer cover was 13.0%.

Changes in conifers within aspen stands were highly variable across the LTB, with some stands experiencing strong increases, some little change, and some were spatially variable, with some pixels increasing faster than others (Figure 3). Across the basin, conifer cover increased significantly through time in 31% of pixels within aspen stands (average slope = 9.2%, average P = 0.0076). Conifer cover decreased significantly through time in 17% of pixels within aspen stands (average slope = -6.1% average P = 0.0101). Conifer cover showed a positive trend through time in another 25% of pixels (average slope = 1.7%) and a negative trend and 27% of aspen stands (average slope = 1.7%), respectively, but trends were not significant at $p < 0.05$. Among the statistically significant increasing pixels, the average rate of increase in conifer cover was 9.7% over the 37-year period. The distribution of increases was skewed, with more smaller values than larger ones and a mode of 6.4%. Among the statistically significant increasing pixels, 2.4% had encroachment rates >25% and 18.2% had encroachment rates >15%. Statistically significant negative pixels had an average of 6.4% over the 37-year period.

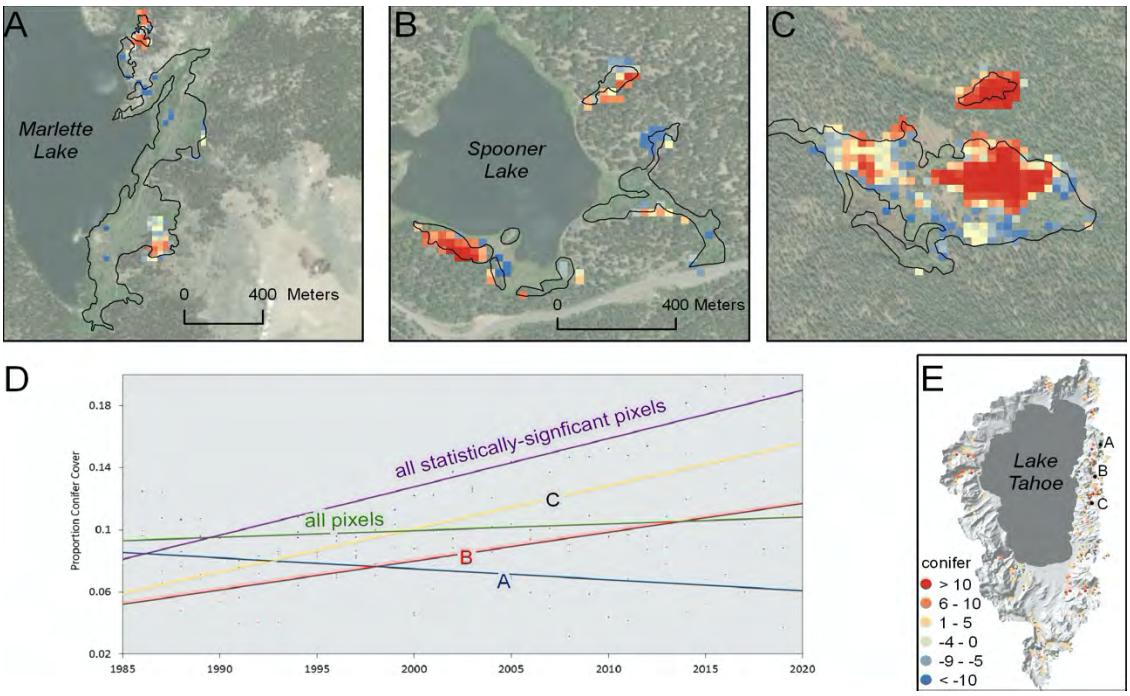

Figure 3. *Predicted statistically-significant increases in conifer cover for three stands on the east side of the LTB A) Marlette Lake, B) Spooner Lake, and C) Logan House Creek. These stands represent a stable aspen stand that has experienced little conifer encroachment (Marlette Lake), a spatially-variable stand that has experienced high levels of encroachment in some areas and low levels in other areas (Spooner Lake), and high conifer encroachment levels throughout most of the stand (Logan House Creek). D) Trends for each of these three stands plus all aspen pixels in the LTB (green line) and all statistically-significant positively trending pixels (purple). The final map shows the average trend in conifer cover within aspen stands for each stand (n=346).*

Abiotic and biotic drivers of conifer encroachment in aspen stands

The predictive model of the rate of conifer cover increase based on abiotic and biotic variables explained 48.3% of the accuracy, compared to Landsat-derived estimates of the rate of conifer cover increase (Figure 4). Model bias was -0.02%. The normalized root mean squared error was 12.1%.

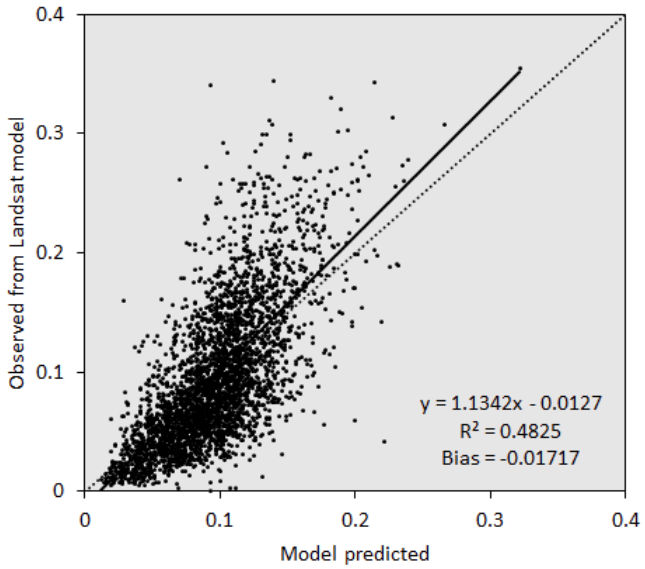

Figure 4. *Relationship between model predicted rate of conifer cover increase in aspen and rate of conifer cover increase. The dashed line is the 1:1 relationship. The solid line is the least-squares line fit to reference data derived from Landsat imagery. Pixels that were not statistically significant or decreased in conifer cover were not considered in the model. Rates represent the proportion change from 1985 to 2020 (36 years).*

The final model of conifer cover trend included 1985 conifer cover plus the first five variables shown in Figure 5 (precipitation, canopy cover at 510 meters, aspen area at 990 meters, mixed conifer cover at 990 meters, silt). The addition of Heat Load Index, temperature, Topographic Position Index, and soil pH did not improve the models and hence were left out of the final model. Among the final variables, precipitation and conifer cover in 1985 were far more important than the other variables as measured by mean decrease accuracy (Figure 6) each explaining 22% of the variance. The aspen area, canopy cover, mixed conifer cover and silt explained 16%, 15%, 14%, and 11% respectively.

The rate of conifer cover increase showed a threshold response to mean annual precipitation with values less than 850 mm being associated with higher levels of conifer encroachment relative to wetter areas (Figure 7a). There was a positive relationship between the rate of conifer cover increase and initial conifer cover in 1985 that saturated at 20% initial conifer cover (Figure 7b). The relationship between the rate of conifer cover increases was positively related to aspen stand area at 990 m scale with larger stands having a partial response indicating that they were more likely to have higher encroachment rates after accounting for all other variables in the model (Figure 7c). The relationship between conifer cover increase and both total canopy cover within 510 m derived from LIDAR and the area of mixed coniferous forest were positive largely linear relationships (Figure 7de). Finally, the relationship between conifer cover increase and percent silt was overall positive but complex (Figure 7f). Many of the largest aspen stands in the basin, such as those near Marlette Lake and in North Canyon had low levels of silt as modeled by the POLARIS data (Chaney et al. 2016).

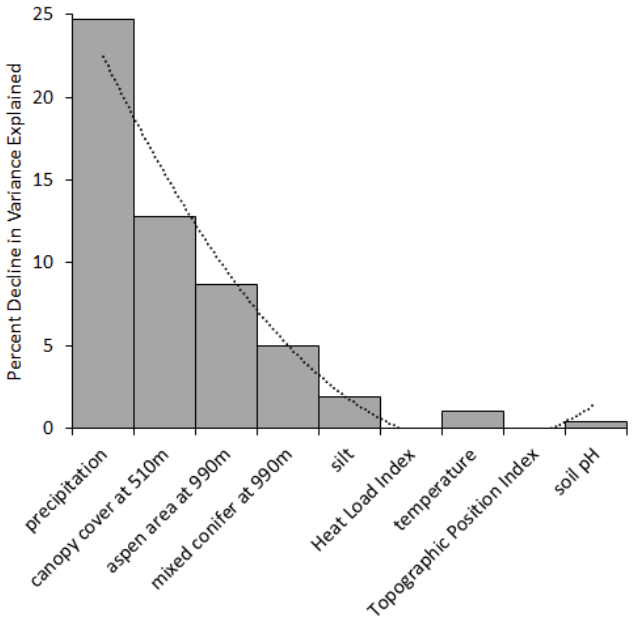

Figure 5. *Contribution of each variable to the variance explained by the model. All models considered conifer cover in 1985 and each model successively builds on the next (e.g., the model that includes canopy cover at 510 m also includes precipitation and conifer cover in 1985). The dashed line is a polynomial that was fitted using the variance explained by all nine models.*

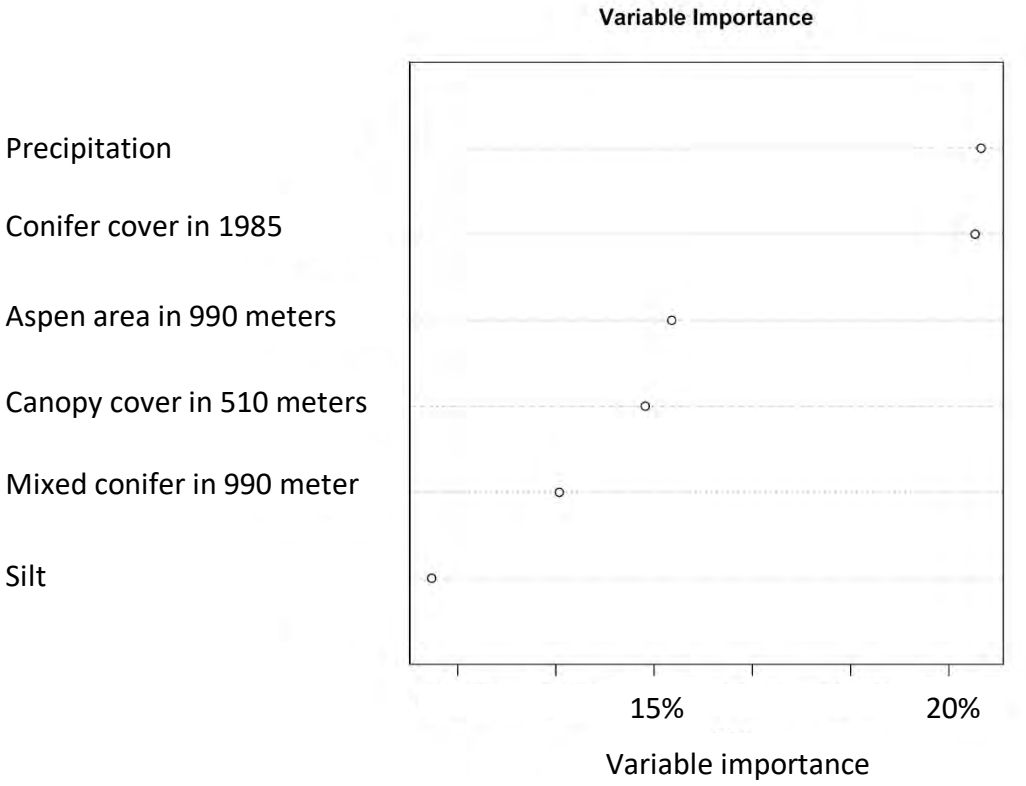

Figure 6. *Variable importance as measured by the mean decrease in accuracy from the Random Forest regression tree model with precipitation, conifer cover in 1985, aspen area within 990 m, canopy cover within 510 m, mixed conifer cover within 990 meters, and silt ranked in order of importance.*

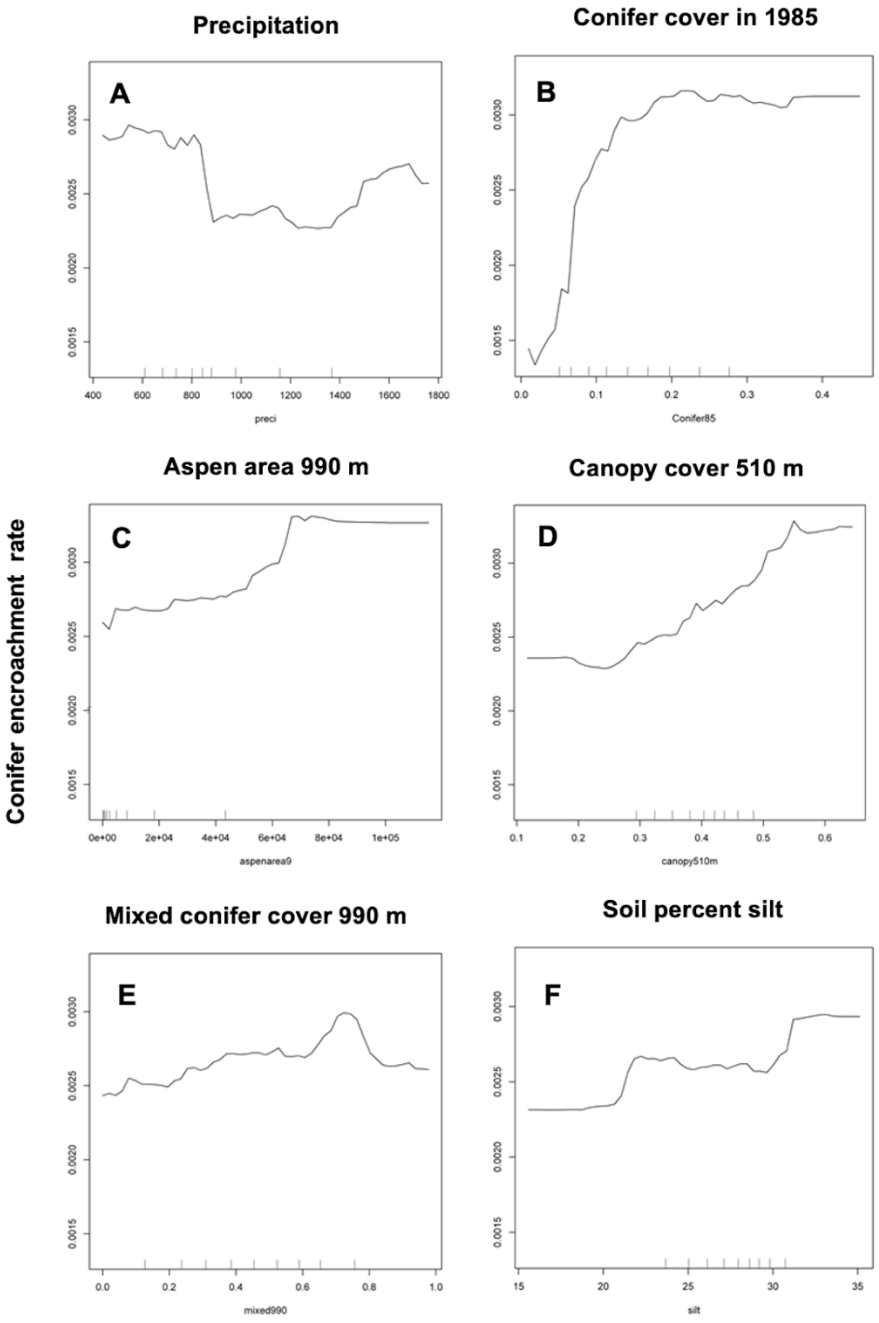

Figure 7. *Partial dependence plots showing the relationship between the estimated rate of conifer encroachment in aspen stands and a) mean annual precipitation, b) conifer cover in 1985, c) area of aspen at the 990-m scale, d) canopy cover at 510 m, e) mixed conifer cover at 990-m, and f) percent silt.*

Environmental conditions among stable and conifer-encroached aspen stands

The model of the environmental conditions predicting stable versus conifer-encroached aspen had an area-under-the-curve (AUC) of the receiver-operating-characteristic (ROC) of 0.88 and a root mean squared error (RMSE) of 0.351. The density histogram (Figure 8) shows 16% overlap between the environmental conditions that predict stable versus conifer-encroached stands with 95% of aspen cells with conifers having a threshold of 0.208 and 100% of aspen cells with conifers having a threshold of 0.006. This results in 44% of the total aspen area being below the 95% threshold and only 1.1% of total area being below the lowest statistically significant conifer increase or totally outside of the environmental envelope in which conifer encroachment occurs.

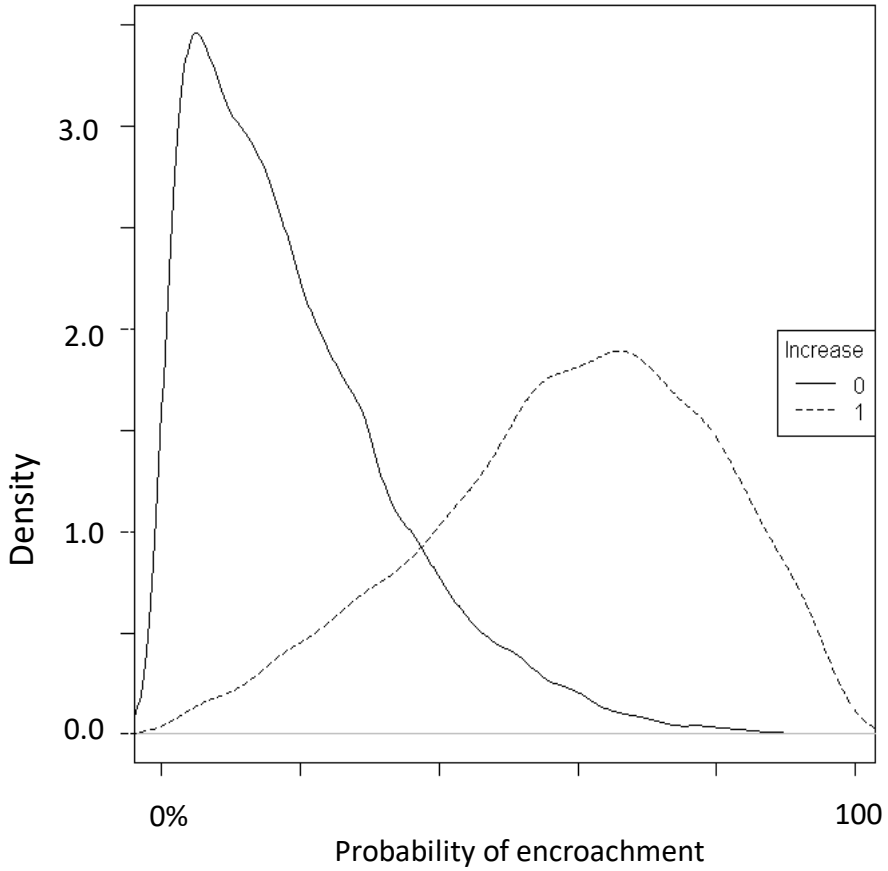

Figure 8. *Density histogram with predicted probability of conifer encroachment on the x-axis and relative density of points on the y-axis. The dashed line shows aspen cells that had statistically-significant levels of conifer encroachment. The solid line shows aspen cells in which the 1985-2020 trend in conifer cover within aspen was either insignificant or negative.*

The final model of conifer encroachment probability included temperature plus the first seven variables shown in Figure 9 (precipitation, canopy cover, aspen area, mixed conifer cover, silt, yellow pine cover, and soil available water content). The addition of soil organic matter and depth to restrictive layer did not improve the models and hence were left out of the final model. Among the final variables in the conifer encroachment model (Figure 10) temperature and precipitation were the most important variables 19 and 18% of the variance respectively. Area of aspen, area of mixed conifer, and area of yellow pine were of secondary importance explaining 12, 12, and 11% of the variance respectively. Silt content, canopy cover, and soil available water content were the least important variables in the model explaining 10, 10 and 9% of the variance, respectively.

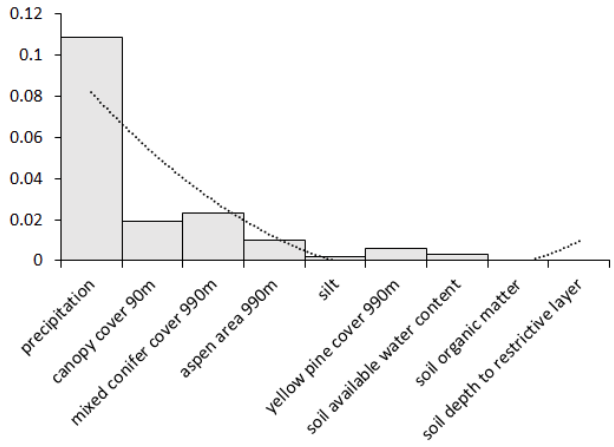

Figure 9. *Contribution of each variable to the variance explained by the model. All models considered temperature and each model successively builds on the next (e.g., the model that includes canopy cover at 990 m also includes temperature and precipitation). The dashed line is a polynomial that was fitted using the variance explained by all nine models.*

The relationship between the probability of conifer encroachment and temperature was positive and linear such that higher temperature sites, for the most part, were more likely to see conifer encroachment compared to cooler sites (Figure 10). There was a negative relationship between the probability of encroachment and precipitation although the relationship appears to be more of a threshold relationship. The relationship between encroachment probability and amount of aspen was the inverse of a unimodal relationship in which pixels with fewer surrounding aspen pixels were more likely to see encroachment than pixels with moderate levels of aspen. Pixels with the highest amounts of aspen had a higher probability of encroachment although the number of very large stands is relatively few in the LTB. The probability of encroachment was positively related to the proportion of yellow pine (*Pinus jeffreyi* and *P. ponderosa*), but had a non-linear relationship increasing to about 5% and then leveling off. The relationship between probability of encroachment and total canopy cover within 90 m was positive and mostly linear. The relationship between probability of encroachment and soil variables were more complex with silt appearing to be the inverse of unimodal relationship and available water content appearing to be positively associated with the probability of encroachment.

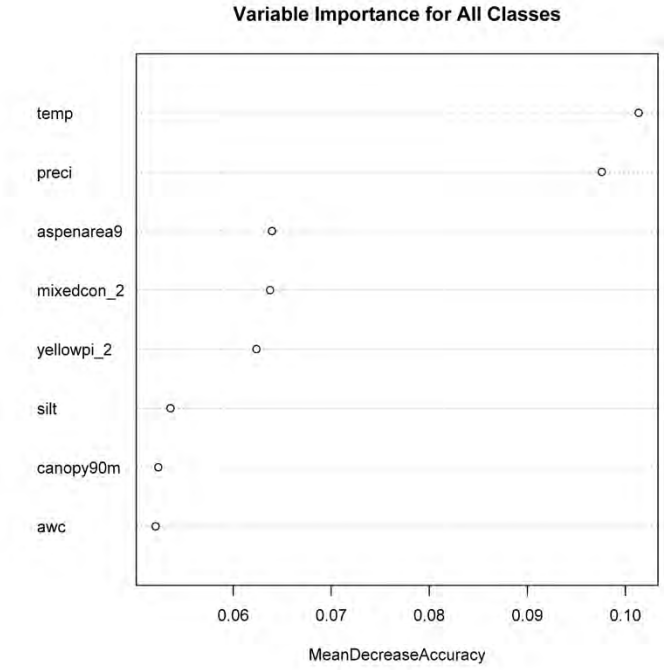

Figure 10. *Variable importance as measured by the mean decrease in accuracy from the Random Forest classification tree model with temperature, precipitation, aspen area within 990 m, mixed conifer cover within 990 m, yellow pine within 990 m, silt, canopy cover within 90 m, and soil available water content.*

Combining our remotely-sensed model of conifer cover with our predictive model of conifer cover increase and our probability of occurrence model allowed us to extrapolate current trends in coniferous encroachment into the future (Figure 11). Our results suggest that there has been a shift in the basin towards higher levels of conifers with a mean of 12.5% in 1986 to a mean of 15.1% in 2020. Extrapolating into the future without considering management actions that may mitigate conifer encroachment rates, we estimate a mean conifer cover in aspen stands of 17.9% in 2056 if we consider both the conifer trend and probability of occurrence. This estimate increases to a mean conifer cover of 23.5% if we only consider the conifer trend across the LTB.

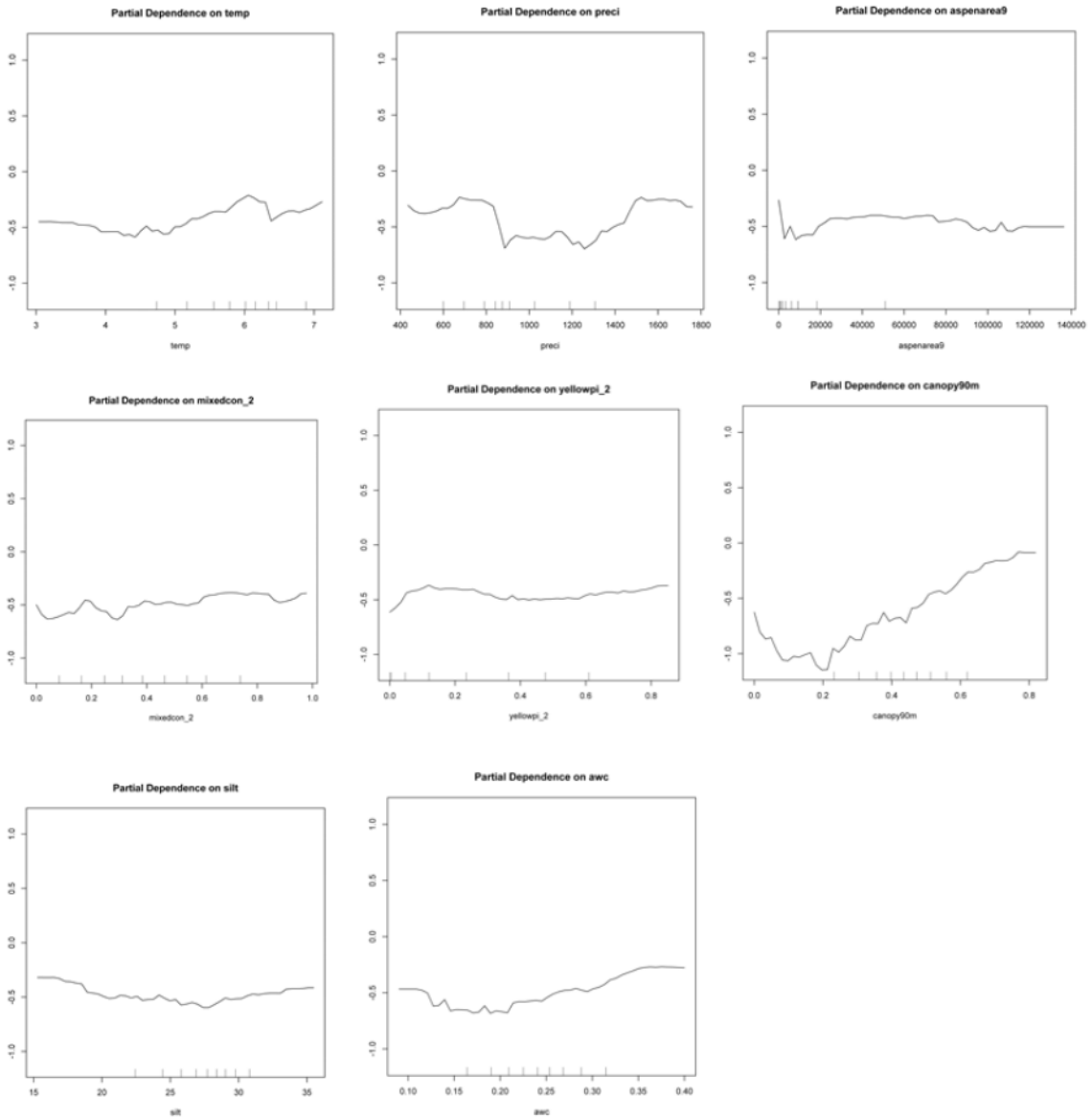

Figure 11. *Partial dependence plots showing temperature, precipitation, area of aspen at the 990 meter scale, mixed conifer cover at 990 meter, yellow pine at 990 meters, canopy cover at 90 meter, percent silt, and soil available water content.*

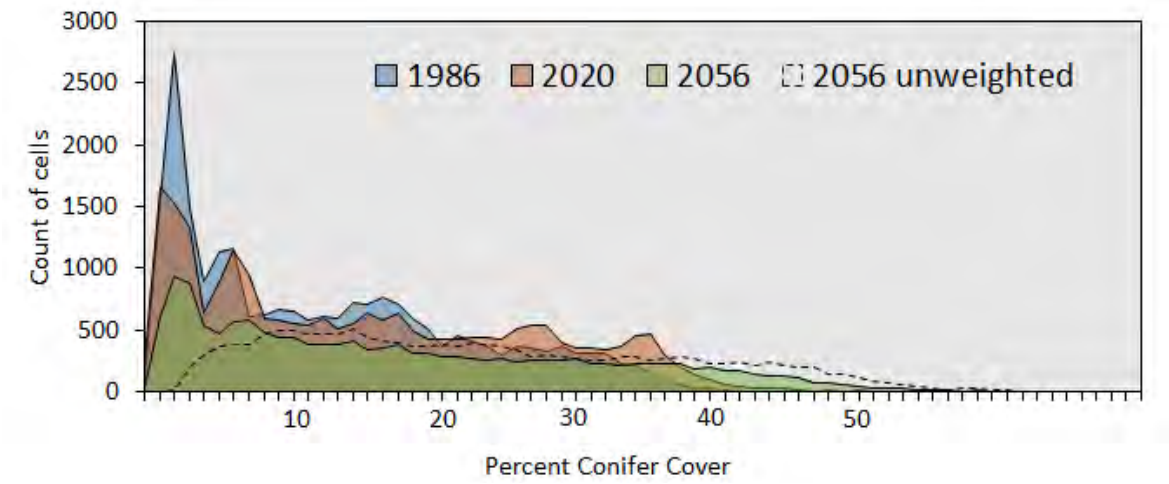

Figure 12. *The relative proportion of conifer cover within aspen stands across the LTB for 1986 (based on remote sensing estimates), 2020 (based on remote sensing estimates), and 2056 estimated by extrapolating the predictive conifer cover increases combined with the probability of occurrence. A second estimate for 2056 (dashed line) is only based on conifer cover increases without considering probability of occurrence.*

Discussion

Dynamics of conifer encroachment in aspen stands

Our findings indicate that conifer cover within aspen stands in the LTB has increased since the 1980s and that the changes are detectable using Landsat imagery. We hypothesize that these patterns will continue in the future if management actions (such as conifer removal) or fire do not limit conifer expansion. By extrapolating current rates of encroachment into the future, we estimate that the average conifer cover in aspen stands in 2055 will be 2.8% to 8.4% higher than in 2020, depending upon the assumptions that are made (Figure 11).

Brewen et al. (2021) used aerial photographs to delineate conifers within aspen at sites in Modoc, Plumas, and Lassen National Forest and found annual encroachment rates of 0.19%, 0.57%, and 0.86% per year. Our annual average rate was 0.24% per year, which is well within the rates that Brewen et al. (2021) estimated for neighboring areas. However, some portions of our study area had rates as high as 1.3% per year. In an aerial photo interpretation study of conifer encroachment between 1952 and 1998 in Lassen Volcanic National Park, McCullough et al. (2013) found conifer cover increased by an average of 1% per year within aspen stands, while aspen cover declined by 0.3% per year during the same period. The spatially heterogeneous nature of conifer encroachment suggests that understanding the abiotic and biotic drivers of conifer expansion into aspen may be critical for effectively allocating limiting funds to restoration activities.

Our findings do not support the idea that there are environments in the LTB that support aspen populations but preclude conifer encroachment without disturbance. Topographic variables, such as slope, Topographic Position Index (Weiss 2001) and Topographic Wetness Index (Beven and Kikby 1979) were not among the variables selected in either the conifer cover or occurrence

models as one might expect for wet meadows or seeps (Strand et al. 2009). However, we acknowledge that topographic proxies for soil wetness can be insufficient in cases where groundwater flows are complex. Although we did not include maps of talus as one of our variables in our models, we would expect talus to be associated with slope, but slope was not found to be important in any of our models. While delineating aspen stands in the LTB, we noted very few aspen in talus, which may suggest that this kind of environmental setting is rare as compared to other regions, or that our mapping methods failed to capture talus aspen. Our model of the probability of conifer encroachment suggested that environmental conditions completely outside the range of conifers may be so rare (1.1%) in the LTB that they are functionally absent from the landscape.

Despite the lack of overlap, there appear to be broad conditions that tend to favor higher rates of conifer encroachment. These conditions include high conifer cover in the initial time (especially greater than 10%), hotter and drier climatic conditions, greater cover of conifers in the surrounding forest, and possibly basaltic soil types (as opposed to granitic soil types that support some of the largest aspen stands in the LTB). Although we did not measure parent material directly, silt content as modeled by the POLARIS soil product (Chaney et al. 2016), was visibly higher in areas with basaltic substrates. We also note that there was a complete absence of aspen stands between Tahoe City and Kings Beach on the north shore of the LTB, an area underlain by basaltic parent material.

Landsat satellite imagery has been used in the past to map understory species in deciduous forests, and likely has great potential across a wide range of deciduous forest ecosystems. Renasco et al. (2007) was able to detect the invasive Amur honeysuckle in the deciduous forests of Ohio using late-autumn Landsat imagery. Atkins et al. (2018) used Landsat TM to map understory *Rhododendron* spp. in West Virginia. They found that the expansion of rhododendron impacted the re-introduction of red spruce, leading to lower levels of regeneration and growth in the spruce. Although we know of no studies to date other than ours that map conifers in aspen stands, Wolter et al. (2012) had success using winter leaf-off imagery to estimate basal area of aspen stems. Winter imagery may offer some advantages over both summer and autumn imagery when it comes to mapping understory species. Conifers in the understory of aspen are unlikely to be visible in summer imagery, and autumn imagery can be affected by the timing of both leaf senescence and leaf loss, which may be related to climatic factors such as frost events and windstorms. Winter imagery may provide optimal contrast between a mostly snowy ground and photosynthetically active coniferous needles in areas like the LTB. We found that using winter imagery in our models lead to decreased interannual variability in conifer cover estimates.

Our maps of aspen stand boundaries represent the first attempt to use high-resolution imagery to create detailed maps of aspen stands on the Nevada side of the LTB. On the California side of the basin, our mapping resulted in smaller average patch sizes (1.27 ha compared to 2.47 ha) compared to the Aspen Delineation Project (Stermer and Burton 2011), likely because of the additional detail in capturing the shape of aspen stands. Our use of multiple image sources, but especially high-resolution leaf-off imagery, contributed to the high fidelity of our data product, and, if confirmed with further field validation, may lead to the discovery of new aspen populations in the LTB. Our use of leaf-off high-resolution aerial photography allowed us to map current cover of conifers within aspen stands and provides a potential baseline to monitor

conifers within aspen. This was achieved using simple GIS software without the need for downloading or processing imagery and can be replicated for other study areas provided that leaf-off imagery is available.

Methodological considerations

Prior to 2008, when the Landsat archive was made publicly available under Landsat Data Policy (Wulder et al. 2012), two-date or three-date change detection studies were commonplace in ecological remote sensing. After the data were made freely available, a wide range of change detection studies began to develop newer methods that were more capable of detecting gradual changes that relied on a greater number of images (Kennedy et al. 2010; Verbesselt et al. 2010; Zhu and Woodcock 2014). Our average estimate of conifer cover expansion in aspen was less than 1% per year, which necessitates the need for approaches that are capable of detecting gradual changes (Vogelmann et al. 2016). Due to the amount of interannual spectral variability and the very gradual rate of change being measured comparing two individual fractional cover maps would likely yield misleading results and should be avoided whereas the use of techniques, such as trend analysis, that use all available years may be much better at detecting gradual change.

Our use of high-resolution imagery (mostly WorldView-2) allowed us to successfully develop accurate maps of conifer cover for 2018. Mapping these changes further back in time from high-resolution imagery may be challenging. For example, most publicly-available high-resolution imagery sources in the United States from the 1980s and 1990s are black and white single-band orthophotos (e.g., National High Altitude Photography Program (NHAP), National Aerial Photography Program (NAPP), National Digital Ortho Program (NDOP) (Godfrey and Kenyon 2017), which may be difficult to identify conifers in or may have seasonality constraints. Moving forward, archival WorldView-2 and other sub-meter satellite images provide an independent source of data that can be used to quantify conifer cover change through time. Coupled with moderate-resolution sensors, such as Landsat and Sentinel, high-resolution imagery has the potential to quantify long-term aspen-conifer dynamics.

Management recommendations and next steps

In addition to identifying many of the abiotic and biotic drivers of conifer expansion in the Lake Tahoe Basin, we have developed spatially-explicit tools that show detailed trends of conifer expansion into aspen stands. These tools employ easy-to-use, interactive and publicly available web sites where spatial data can be viewed and downloaded without need of GIS software. Furthermore, GIS users can interactively stream the data directly into the platform of their choice (e.g., ArcMap, QGIS, ArcGIS Pro), while maintaining our symbology and labeling. The URL for our conifer expansion webmap is https://arcg.is/1G95G8, whereas our maps for aspen stands, conifer cover within aspen, and interactive public comment layers are at https://arcg.is/aWbir. These data are available now and can be put to use by land managers. Finally, we have developed a set of predictive maps for the year 2055, which are available to land managers and the public at https://arcg.is/0vXuSP0. These maps provide lower and higher estimates of future conifer cover in the LTB that depend upon the assumptions made.

Moving forward, we intend to use the above interactive maps to create an ArcGIS StoryMap to explain how aspen stands in the LTB are changing through time. The ArcGIS StoryMap format combines interactive web GIS with graphs, photographs, and text to provide context and offer more in-depth explanations. Managers can share the StoryMaps with colleagues and the public to highlight the importance of this issue and provide real-world context for this critical issue.

In addition to the web-based products mentioned, we have been in discussion with the LTB Management Unit of the U.S. Forest Service on developing a decision-support tool that will integrate the costs and benefits of where to conduct conifer-removal activities. Treatment criteria will include outputs from this work, such as existing conifer cover, rate of past conifer trend, and risk of future conifer trend, combined with logistical costs such as slope, access, and proximity to riparian zones. The decision support system will also incorporate added benefits having to do with the spatial context of aspen stands relative to other aspen stands. For example, small aspen stands that are adjacent to larger intact ones may be prioritized over smaller more-isolated stands surrounded by conifers.

Conclusion

In this study, we have used remote-sensing approaches to document the distribution of aspen and encroaching conifers in the LTB. Our goal was to quantify rates of conifer encroachment in aspen stands over the past 35 years, identify the biotic and abiotic factors that predict these rates, and determine whether environments exist that support aspen populations but preclude conifers.

The research summarized here shows that conifers have been expanding into aspen stands since the mid 1980s and, without management intervention, we project that this encroachment will continue to increase across most of the LTB, thereby threatening the unique habitats and ecosystem services that aspen provides. Our hope is that the set of interactive, web-based tools that we have developed will aid land managers in their efforts to identify aspen stands throughout the LTB that are most susceptible to conifer encroachment, and therefore in need of management action.

Literature Cited

Allen, C.D., D.D. Breshears, N.G. McDowell. 2015. On underestimation of global vulnerability to tree mortality and forest die-off from hotter drought in the Anthropocene. Ecosphere 6:art129.

Allen, C.D., A.K. Macalady, H. Chenchouni, et al. 2010. A global overview of drought and heat-induced tree mortality reveals emerging climate change risks for forests. Forest Ecology and Management 259:660–684.

Atkins, J. W., Epstein, H. E., & Welsch, D. L. 2018. Using Landsat imagery to map understory shrub expansion relative to landscape position in a mid-Appalachian watershed. Ecosphere, 9(10), e02404.

Bailey, J. K., & Whitham, T. G. 2002. Interactions among fire, aspen, and elk affect insect diversity: reversal of a community response. Ecology, 83(6), 1701-1712.

Berrill and Dagley. 2012. Geographic patterns and stand variables influencing growth and vigor of *Populus tremuloides* in the Sierra Nevada (USA). ISRN Forestry 2012: 1:9.

Berrill, J.P., C.M. Dagley, S.A. Coppeto, and S.E. Gross. 2017. Curtailing succession: Removing conifers enhances understory light and growth of young aspen in mixed stands around Lake Tahoe, California and Nevada, USA. Forest Ecology and Management 400:511-522.

Beven, K. J. & Kirkby, M. J. 1979. A physically based, variable contributing area model of basin hydrology. Hydrological Sciences Journal, 24(1), 43-69.

Bonan, G.B. 2008. Forests and climate change: forcings, feedbacks, and the climate benefits of forests. Science 320:1444–1449.

Breshears, D.D., N.S. Cobb, P.M. Rich, et al. 2005. Regional vegetation die-off in response to global-change-type drought. Proceedings of the National Academy of Sciences 102:15144–15148.

Carlson, D., P. Reich, and L. Frelich. 2011. Fine-scale heterogeneity in overstory composition contributes to heterogeneity of wildfire severity in southern boreal forest. Journal of Forest Research 16:203-214.

Chaney, N. W., Wood, E. F., McBratney, A. B., Hempel, J. W., Nauman, T. W., Brungard, C. W., & Odgers, N. P. 2016. POLARIS: A 30-meter probabilistic soil series map of the contiguous United States. Geoderma, 274, 54-67.

Dagley, C.M., J.P. Berrill, S.A. Coppeto, and A.K. Eschtruth. 2020. Understory responses to restoration in aspen-conifer forests around the Lake Tahoe Basin: residual stand attributes predict recovery. Restoration Ecology 28(3):603-611.

ESRI. (2019) Spatial Analyst Extension for ArcGIS Software Version 10.7.1. Environmental Systems Research Inc. Redlands, CA, USA.

Enders, M.S. (2021) Avian Impacts of White Satin Moth Defoliation in Tahoe Aspen. Project 04.01.01.0134. Lake Tahoe Environmental Improvement Program. Available at https://www.laketahoeinfo.org/Project/Detail/4150.

Evans, J.S. 2020. spatialEco: Spatial Analysis and Modelling Utilities, version1. 3-1. CRAN, R Core Team: Cary, CA, USA.

Filippelli, S. K., Falkowski, M. J., Hudak, A. T., Fekety, P. A., Vogeler, J. C., Khalyani, A. H., ... & Strand, E. K. 2020. Monitoring pinyon-juniper cover and aboveground biomass across the Great Basin. Environmental Research Letters, 15(2), 025004.

Filippelli, S. K., Vogeler, J. C., Falkowski, M. J., & Meneguzzo, D. M. 2020. Monitoring conifer cover: Leaf-off lidar and image-based tracking of eastern redcedar encroachment in central Nebraska. Remote Sensing of Environment, 248, 111961.

Huang, C-Y., W.R.L. Anderegg. 2012. Large drought-induced aboveground live biomass losses in southern Rocky Mountain aspen forests. Global Change Biology 18:1016–1027.

Huntington, J.L., K.C. Hegewisch, B. Daudert, C.G. Morton, J.T. Abatzoglou, D.J. McEvoy, and T. Erickson. 2017. Climate engine: Cloud computing and visualization of climate and remote sensing data for advanced natural resource monitoring and process understanding. Bulletin of the American Meteorological Society 98(11):2397-2410.

Gao, B.C. 1996. NDWI—A normalized difference water index for remote sensing of vegetation liquid water from space. Remote Sensing of Environment 58(3): 257-266.

Gitlin, A. R., Sthultz, C. M., Bowker, M. A., Stumpf, S., Paxton, K. L., Kennedy, K., ... & Whitham, T. G. (2006). Mortality gradients within and among dominant plant populations as barometers of ecosystem change during extreme drought. *Conservation Biology*, *20*(5), 1477-1486.

Godfrey, B. and J. Kenyon. 2017. The USDA's NAIP imagery in Idaho: A decade of evolving partnerships to improve access. Library Trends 65(3):414-428.

Google Inc. (2018) Google Earth Pro Basemap. WorldView-2 imagery November 16, 2018. DigitalGlobe Inc. Last accessed 10/24/2019.

Gorelick, N., M. Hancher, M. Dixon, S. Ilyushchenko, D. Thau, and R. Moore. 2017. Google Earth Engine: Planetary-scale geospatial analysis for everyone. Remote Sensing of Environment, 202:18-27.

Jones, B.E., T.H. Rickman, A. Vazquez, Y. Sado, and K.W. Tate. 2005. Removal of encroaching conifers to regenerate degraded aspen stands in the Sierra Nevada. Restoration Ecology 13: 373-379.

Kashian, D.M., W.H. Romme, and C.M. Regan. 2007. Reconciling divergent interpretations of quaking aspen decline on the northern Colorado Front Range. Ecological Applications 17(5):1296-1311.

Kennedy, R.E., S. Andréfouët, W.B. Cohen, C. Gómez, P. Griffiths, M. Hais, ... and Z. Zhu. 2014. Bringing an ecological view of change to Landsat-based remote sensing. Frontiers in Ecology and the Environment 12(6):339-346.

Kennedy, R.E., Z. Yang, and W.B. Cohen. 2010. Detecting trends in forest disturbance and recovery using yearly Landsat time series: 1. LandTrendr—Temporal segmentation algorithms. Remote Sensing of Environment 114(12):2897-2910.

Krasnow, K.D., A.S. Halford, and S.L. Stephens. 2012. Aspen restoration in the eastern Sierra Nevada: effectiveness of prescribed fire and conifer removal. Fire Ecology 8(3):104-118.

Krasnow, K.D. and S.L. Stephens. 2015. Evolving paradigms of aspen ecology and management: impacts of stand condition and fire severity on vegetation dynamics. Ecosphere 6(1):1-23.

Kuhn, T.J., H.D. Safford, B.E. Jones, and K.W. Tate. 2011. Aspen (*Populus tremuloides*) stands and their contribution to plant diversity in a semiarid coniferous landscape. Plant Ecology, 212(9):1451-1463.

Landhäusser, S.M., D. Deshaies, and V.J. Lieffers. 2010. Disturbance facilitates rapid range expansion of aspen into higher elevations of the Rocky Mountains under a warming climate. Journal of Biogeography 37:68-76.

Landhäusser, S.M., B.D. Pinno, and K.E. Mock. 2019. Tamm Review: Seedling-based ecology, management, and restoration in aspen (*Populus tremuloides*). Forest Ecology and Management. 432: 231-254.

Liaw, A. and M. Wiener. 2002. Classification and regression by randomForest. R news, 2(3):18-22.

Manley, P.N. et al. 2000 Biological Integrity. In: Murphy, D.D., Knopp, C.M. (eds.). Lake Tahoe Watershed Assessment: Volume I. Gen. Tech. Rep. PSW-GTR-175. Pacific Southwest Research Station, USDA Forest Service, Albany, CA.

McCullough, S.A., A.T. O'Geen, M.L. Whiting, D.A. Sarr, and K.W. Tate. 2013. Quantifying the consequences of conifer succession in aspen stands: decline in a biodiversity-supporting community. Environmental Monitoring and Assessment 185:5563-5576.

McCune, B. and D. Keon. 2002. Equations for potential annual direct incident radiation and heat load. Journal of Vegetation Science, 13(4):603-606.

Pan, Y., R.A. Birdsey, J. Fang, et al. 2011. A large and persistent carbon sink in the world's forests. Science 333:988–993.

Pierce, A.D. and A.H. Taylor. 2010. Competition and regeneration in quaking aspen-white fir (*Populus tremuloides-Abies concolor*) forests in the Northern Sierra Nevada, USA. Journal of Vegetation Science 21(3):507-519.

Rehfeldt, G.E., D.E. Ferguson, and N.L. Crookston. 2009. Aspen, climate, and sudden decline in western USA. Forest Ecology and Management 258:2353–2364.

Resasco, J., A.N. Hale, M.C. Henry, and D.L. Gorchov. 2007. Detecting an invasive shrub in a deciduous forest understory using late-fall Landsat sensor imagery. International Journal of Remote Sensing 28(16):3739-3745.

Richardson, T. W., and S.K. Heath. 2004. Effects of conifers on aspen-breeding bird communities in the Sierra Nevada. Transactions of the Western Section of the Wildlife Society 40:68-81.

Richardson, T. W., and S.B. Vander Wall. 2007. Yellow pine chipmunks cannot climb quaking aspens: implications for avian nest site selection. Western North American Naturalist 67(2):251-257.

Ripple, W.J. and E.J. Larsen. 2001. The role of postfire woody debris in aspen regeneration. Western Journal of Applied Forestry 16(2):61-64.

Romsos, J.S. (2011) LiDAR remote sensing data collection: Lake Tahoe. August, 24, 2010. https://portal.opentopography.org/datasetMetadata?otCollectionID=OT.032011.26910.1. Last accessed: 2/18/2018.

Sappington, J.M., K.M. Longshore, and D.B. Thompson. 2007. Quantifying landscape ruggedness for animal habitat analysis: a case study using bighorn sheep in the Mojave Desert. The Journal of Wildlife Management 71(5):1419-1426.

Shepperd, W.D., P.C. Rogers, D. Burton, and D.L. Bartos. 2006. Ecology, Biodiversity, Management, and Restoration of Aspen in the Sierra Nevada. General Technical Report RMRS-GTR-178. USDA Forest Service, Rocky Mountain Research Station, Fort Collins, Colorado, USA.

Smith, J., R. Laven, and P. Omi. 1993. Microplot sampling of fire behavior on *Populus tremuloides* stands in north-central Colorado. International Journal of Wildland Fire 3:85-94.

Strand, E.K., L.A. Vierling, S.C. Bunting, and P.E. Gessler. 2009. Quantifying successional rates in western aspen woodlands: Current conditions, future predictions. Forest Ecology and Management 257:1705-1715.

Stephens, S.L., R.E. Martin, and N.E. Clinton. 2007. Prehistoric fire area and emissions from California's forests, woodlands, shrublands and grasslands. Forest Ecology and Management 251:205-216.

Trumbore, S., P. Brando, H. Hartmann. 2015. Forest health and global change. Science 349:814–818.

Tucker, C.J. 1979. Red and photographic infrared linear combinations for monitoring vegetation. Remote Sensing of Environment, 8(2), 127-150.

Turner, M.G., W.H. Romme, R.A. Reed, and G.A. Tuskan. 2003. Post-fire aspen seedling recruitment across the Yellowstone (USA) landscape. Landscape Ecology 18:127-140.

USDA (2014) Soil Survey Geographic (SSURGO) Database for the Conterminous United States. United States Department of Agriculture, Natural Resources Conservation Service. Available online at: http://datagateway.nrcs.usda.gov

USDA. (2017) National Agriculture Imagery Program. August 8, 2017. US Department of Agriculture Farm Services Agency. Last accessed 10/24/2019.

van Mantgem, P.J., N.L. Stephenson, J.C. Byrne, et al. 2009. Widespread increase of tree mortality rates in the western United States. Science 323:521–524.

Vogelmann, J.E., B. Tolk, and Z. Zhu. 2009. Monitoring forest changes in the southwestern United States using multitemporal Landsat data. Remote Sensing of Environment, 113(8), 1739-1748.

Wayman, R.B. and M. North. 2007. Initial response of a mixed-conifer understory plant community to burning and thinning restoration treatments. Forest Ecology and Management 239:32-44.

Weiss, A. 2001. Topographic position and landforms analysis. In Poster presentation, ESRI user conference, San Diego, CA (Vol. 200).

Wolter, P. T., Berkley, E. A., Peckham, S. D., Singh, A., & Townsend, P. A. 2012. Exploiting tree shadows on snow for estimating forest basal area using Landsat data. Remote Sensing of Environment, 121, 69-79.

Worrall J.J., L. Egeland, T. Eager, et al. 2008. Rapid mortality of *Populus tremuloides* in southwestern Colorado, USA. Forest Ecology and Management 255:686–696.

Worrall J.J., S.B. Marchetti S.B., L. Egeland, et al. 2010. Effects and etiology of sudden aspen decline in southwestern Colorado, USA. Forest Ecology and Management 260:638–648.

Worrall J.J., G.E. Rehfeldt, A. Hamann, E.H. Hogg, S.B. Marchetti, M. Michaelian, and L.K. Gray. 2013. Recent declines of *Populus tremuloides* in North America linked to climate. Forest Ecology and Management, 299, 35–51.

Wulder, M. A., Loveland, T. R., Roy, D. P., Crawford, C. J., Masek, J. G., Woodcock, C. E., ... & Zhu, Z. 2019. Current status of Landsat program, science, and applications. Remote Sensing of Environment, 225, 127-147.

Yang, J., P.J. Weisberg, and N.A. Bristow. 2012. Landsat remote sensing approaches for monitoring long-term tree cover dynamics in semi-arid woodlands: Comparison of vegetation indices and spectral mixture analysis. Remote Sensing of Environment, 119, 62-71.

Zhu, Z. and C.E. Woodcock. 2014. Continuous change detection and classification of land cover using all available Landsat data. Remote sensing of Environment, 144, 152-171.

Zegler T.J., M.M. Moore, M.L. Fairweather, et al. 2012. *Populus tremuloides* mortality near the southwestern edge of its range. Forest Ecology and Management 282:196–207.